

# Effects of torrefaction on the physicochemical characteristics of sawdust and rice husk and their pyrolysis behavior by TGA and Py-GC/MS

Wenfei Cai <sup>†,‡,§</sup>, Antzela Fivga <sup>†,‡,§</sup>, Ossi Kaario <sup>▽</sup>, Ronghou Liu <sup>\*,†,‡</sup>

<sup>†</sup>. Biomass Energy Engineering Research Centre, School of Agriculture and Biology, Shanghai Jiao Tong University, 800 Dongchuan Road, Shanghai 200240, PR China

<sup>‡</sup>. Key Laboratory of Urban Agriculture (South), Ministry of Agriculture, 800 Dongchuan Road, Shanghai 200240, PR China

<sup>§</sup>. Bioenergy Research Group, European Bioenergy Research Institute (EBRI), Aston University, Aston Triangle, Birmingham B4 7ET, United Kingdom

<sup>▽</sup>. Department of Mechanical Engineering, School of Engineering, Aalto University, 00076 Aalto, Finland

## Abstract

The purpose of this research is to investigate the torrefaction behavior of sawdust and rice husk and the torrefaction influence on the thermal chemical properties of the two kinds of biomass, using three different temperature levels 200-220 °C, 240-260 °C, and 280-300 °C for 1 hour. Results showed that the weight loss of sawdust was more significant than that of rice husk in 280-300 °C, which was 27.72% and 18.33%, respectively. The energy yields decreased with the increase of the torrefaction temperature, which were 77.63% and 89.38% for sawdust and rice husk in 280-300 °C, respectively. After torrefaction in 280-300 °C, HHV of sawdust increased from 20.84 MJ/kg to 22.38

---

\* Corresponding author: Ronghou Liu, E-mail: liurhou@sjtu.edu.cn, Tel: 0086 21 34205744

MJ/kg, and that of rice husk changed from 17.07 MJ/kg to 18.68 MJ/kg. Hemicellulose was the most reactive material in the process of devolatilisation by TGA. The degradation temperature of cellulose occurred at 270-360 °C and 250-345 °C for sawdust and rice husk, respectively. Py-GC/MS data showed that the process of torrefaction reduced the levels of alcohols, ketones, aldehydes, acids, esters, and furans of the pyrolysis products for both kinds of biomass. Phenols content in sawdust was increased from 13.84% to 15.68% after torrefaction, and that for rice husk was increased from 10.94% to 13.66% after torrefaction. Systematic characterization of sawdust and rice husk in the surface morphology, energy yield, lignocellulose components composition, and thermal cracking performance before and after the torrefaction process was carried out, which enhances the practicability of using the torrefied biomass as a fuel and facilitates the application of biomass as a promising alternative clean energy.

Keywords:

Torrefaction; sawdust; rice husk; thermogravimetric analysis (TGA); pyrolysis-gas chromatography/mass spectrometry (Py-GC/MS)

## 1. Introduction

With the rapid depletion of the conventional energy resources such as coal, petroleum or natural gas,<sup>1</sup> the continuous fluctuation of the energy prices, the increasing risk of the environmental threats,<sup>2</sup> global efforts are devoted to find renewable, sustainable, and environmental-friendly energy.<sup>3</sup> In the arena of alternative energy investigation, bioenergy bears incomparable advantages in contrast to many other forms of renewable energy like solar, wind, hydropower, ocean, and

geothermal energy, not only because bioenergy is the most common form of renewable energy,<sup>4</sup> but also because the final products from e.g. bioethanol,<sup>5</sup> bio-oil, and syngas are compatible to the existing petrochemical industry. However, some undesirable characteristics of biomass, such as low bulk density, low energy density, high moisture content, high logistics cost, and heterogeneous nature, seriously compromised the development in bioenergy.<sup>6, 7</sup> In recent years, torrefaction, a promising thermal pretreatment method,<sup>8</sup> exhibits some positive effects.

Torrefaction, a mild thermolysis process, subjects the feedstock to a thermal treatment at relatively low temperatures of 200-300 °C in an inert atmosphere. Torrefaction may reduce the moisture content, atomic O/C ratio. In addition, it can reduce logistic costs of the feedstock when it is applied with the technology like pelletisation. It can also intensify the heating value, hydrophobicity, grindability, flowability, and homogeneity of the biomass.<sup>8, 9</sup> All these changes improve solid fuel qualities<sup>10</sup> and combustion features, which make the torrefied sample become more storable, combustible, and attractive for a novel renewable fuel. In the research of Bridgeman *et al.*,<sup>11</sup> both volatile and char combustion of the torrefied sample become more exothermic compared to the raw biomass, and depending on the severity of the torrefaction conditions, the torrefied fuel can contain up to 96% of the original energy content on a mass basis. Arias *et al.*<sup>6</sup> compared the grindability of raw biomass and the treated samples and observed an improvement in the grindability characteristics after the torrefaction process. Pimchuai *et al.*<sup>12</sup> found that combustible properties of sawdust, rice husk, and two other agriculture residues were enhanced by the torrefaction process. In addition, Tooran *et al.*<sup>13</sup> investigated the torrefaction effect on the chemistry of birch wood under 240-280 °C and found that 240 °C is sufficient to degrade hemicelluloses and cellulose degradation begins at 270 °C, but for lignin degradation begins at 240

°C. Prins *et al.*<sup>14</sup> found that torrefaction can increase heating value of the biomass by decomposing the reactive hemicellulose fraction. The weight loss kinetics for torrefaction can be described as a two-step reaction, where the fast initial step may be representative of hemicellulose decomposition. Chen *et al.*<sup>15</sup> investigated the property and structure variations of three kinds of agricultural wastes, including sawdust and rice husks, under torrefaction pretreatment and found that when the temperature and torrefaction time increase the property of the torrefied biomass is like high-volatile coal.

Up to date, despite lots of impressive torrefaction research focusing on improving the fuel properties of the biomass, the comparative study on the variation of different kinds of biomasses under distinct torrefaction conditions is not sufficient. Especially how the torrefaction conditions affect lignocellulosic components (hemicellulose, cellulose, and lignin) of the two kinds of raw materials, including sawdust and rice husk, changes and weight loss is inadequately known at the moment. Thereby, a systematic analysis of the differences in the surface morphology, energy yield, material composition (especially lignocellulose components), and thermal cracking performance between woody plant (sawdust) and annual herbaceous plant (rice husk) before and after the torrefaction process is investigated. Accordingly, the objectives of the present study can be formulated as: 1) investigate the torrefaction behavior of two kinds of raw materials, including sawdust and rice husk, under three different temperature levels of 200-220 °C, 240-260 °C, and 280-300 °C, representing light, mild, and severe torrefaction; 2) perform detailed lignocellulosic components analysis of the original feedstocks and the torrefied biomass; 3) analyze the thermal cracking characteristics of the raw materials and the torrefied biomass by TGA and Py-GC/MS; and 4) evaluate the application of the torrefied biomass as a renewable fuel. This work provides valid

reference and technical support for biomass torrefaction and its potential utilization.

## 2. Experimental methods

### 2.1. Feedstock preparation

Sawdust (from pine wood) and rice husk, with characteristics of particle size between 0.178 and 0.599 mm, were collected from Chuanghui Furniture (Shanghai) Co., Ltd. and a rice processing factory in Songjiang Park, Shanghai, P. R. China, respectively. All the biomass samples were dried in an open area for 5 days before being stored at room temperature on site, using air tight containers, to provide a basis for experiments.

### 2.2. Biomass pretreatment by torrefaction

The torrefaction behavior of two kinds of raw materials, sawdust and rice husk, was investigated under three different temperature levels of 200-220 °C, 240-260 °C, and 280-300 °C, representing light, mild, and severe torrefaction. The temperature was controlled by a computer. The temperature was set at 210, 250, 290 °C. If the temperature is lower or higher than the desired temperature of 10 °C, the heater will work or be shut down, automatically. In each run, approximately 25 grams of sawdust or rice husk was subject to torrefaction (atmospheric pressure) at three different temperature severities 200-220 °C, 240-260 °C, and 280-300 °C for 1 hour. A muffle oven modified to accommodate a gas inlet and outlet, fitted with a one way valve system, was used. The torrefaction process was carried out in an inert atmosphere using nitrogen gas, at a constant flow rate of 50 l/h. A high gas flow rate was used to ensure a constant gas flush. Prior to commencing the torrefaction process, the system was purged for 20 minutes to remove air from the oven. The oven was then heated at a heating rate of 10 °C/min to the desired torrefaction temperature. This temperature was then held for 1 hour before being turned off. Then the unit was allowed to cool under the same gas

flow rate conditions to approximately 100 °C. Then the samples were transferred to a desiccator and cooled to the room temperature. Once cooled, the treated feedstock was weighed and characterized. Schematic diagram of the torrefaction unit is shown schematically in Figure 1. To ensure uniform results, the torrefaction process was repeated twice and average values were taken.

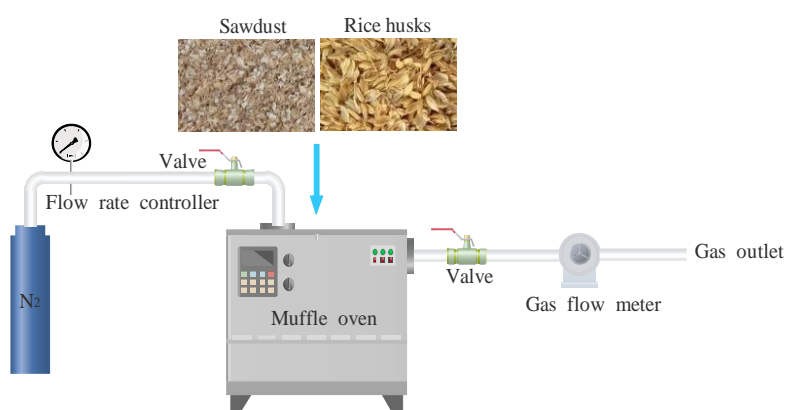


Figure 1. Schematic diagram of the torrefaction unit

### 2.3. Material analysis

The micrographs were taken using a scanning electron microscope (FEI Sirion 200). Observations were reported at three levels of magnification: 0-20  $\mu\text{m}$ , 0-50  $\mu\text{m}$ , and 0-500  $\mu\text{m}$ . The proximate analysis of all the samples was performed in accordance with the standard procedure of American Society for Testing and Materials (ASTM), ASTM E 1756-08 for moisture content, ASTM E 1755-01 for ash content and ASTM E872-82 for volatile matter. Ultimate analysis of the samples was performed to get the elemental content of carbon, hydrogen, and nitrogen using an Elemental Analyzer (Model Vario EL III). The elemental content of oxygen was calculated by difference. The inorganic content was determined by inductively coupled plasma-optical emission spectroscopy (ICP–OES) with the method of ICP general rule JY/T015-1996. Those analysis were done twice and the average value was recorded. The following equations were used to calculate the higher<sup>16</sup> (EQ1) and lower<sup>17</sup> (EQ2) heating values:

$$\text{HHV} = 0.3491\text{C} + 1.1783\text{H} + 0.1005\text{S} - 0.1034\text{O} - 0.0151\text{N} - 0.0211\text{A} \quad (\text{MJ/kg}) \quad (\text{EQ1})$$

$$\text{LHV} = \text{HHV} - 2.442 \times 8.936 \times (\text{H}/100) \quad (\text{MJ/kg}) \quad (\text{EQ2})$$

where HHV and LHV represent higher and lower heating values on dry basis. C, H, O, N, S, and A represent carbon, hydrogen, oxygen, nitrogen, sulphur, and ash contents of the material, respectively, expressed in mass percentages on dry basis.

In regard to the fiber analysis, the compositional content (hemicellulose, cellulose, lignin, insoluble ash, and cell content-proteins, fat, soluble carbohydrate and soluble ash) of the untreated and pretreated (torrefaction) samples were analyzed, following the Van-Soest procedure with the VELP scientifica FIWE raw fiber extractor (6-position raw fiber extractor). In TGA experiment, the sample was crushed to small particles (particle size <180 µm) to minimize the temperature gradients within the sample. The TGA with the heating rate of 10 °C/min was executed by a thermogravimetry (PerkinElmer Pyris 1 TGA) where the temperature ranged from 25 to 575 °C. All samples (approximately 3-5 mg) were pyrolyzed where the carrier gas (nitrogen) flow rate was 25 ml/min and held at 575 °C for 15 minutes. The untreated biomass and the biomass after torrefaction at 280-300 °C for 1 h were performed by Py-GC-MS (CDS 5200 pyrolyser, PerkinElmer Clarus 680 GC-MS). Dried sample is placed in a 20 mm quartz tube between two quartz wool plugs. Pyrolysis conditions: dried sample 1.5 mg, temperature at 550 °C, heating rate 500 °C/s, period 30 s. Pyrolysis vapor is trapped using a Tenax®-2 trap maintained at 45 °C, then desorbed at 280 °C (1 minute) and then transferred via a heated transfer line (310 °C) onto the GC column via an injection port kept at 300 °C. Separation is carried out on a PerkinElmer Elite-1701 column (30 m X 0.25 mm, film thickness 0.25 µm, split ratio 1:50). GC conditions: time period 50 minutes, molecular mass range m/z = 35-300, carrier gas helium, gas flow rate 15 ml/min, scan time 0.35 s, mass spectral detection

library (NIST05 MS library).

### 3. Results and discussion

#### 3.1. Surface morphology

Figure 2 shows the observations of raw material and torrefied biomass at the torrefaction temperatures of 200-220 °C, 240-260 °C, and 280-300 °C. It can be seen from the Figure 2 that with the increased torrefaction temperature, the color of sawdust and rice husk changed from light yellow to dark brown, due to the carbonization of the biomass surface. Sawdust was more sensitive to the increasing temperature, especially at the torrefaction temperatures of 240-260 °C, where the color of the torrefied sawdust was significantly darker than that of the torrefied rice husk. In addition, to gain a further understanding of the impact of torrefaction on the biomass, the morphological differences between all samples were tested by the scanning electron microscopy (SEM) technique. SEM micrographs of raw material and torrefied biomass are shown in Figure 3. The images have been amplified by factors of 100, 1000, and 2000.

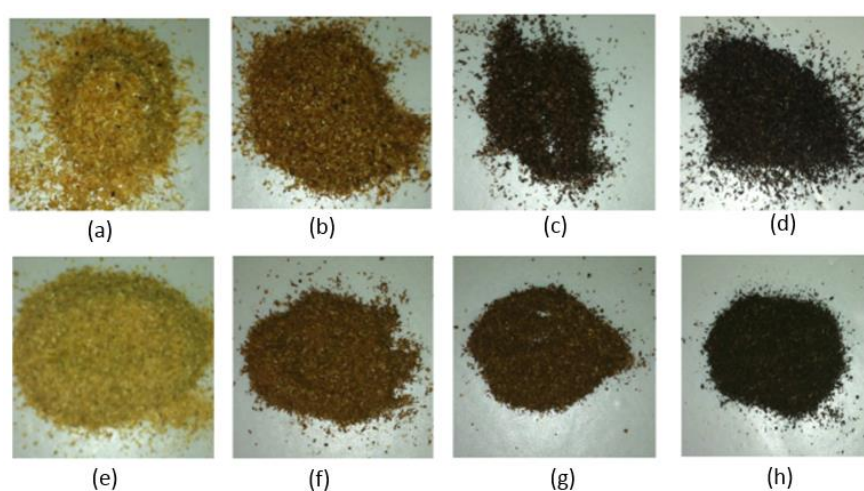


Figure 2. Observations of raw material and torrefied biomass at the torrefaction temperatures of 200-220 °C, 240-260 °C, and 280-300 °C

(a) sawdust, raw material; (b) sawdust, 200-220 °C; (c) sawdust, 240-260 °C; (d) sawdust, 280-300 °C; (e) rice husk, raw material; (f) rice husk, 200-220 °C; (g) rice husk, 240-260 °C; (h) rice husk,

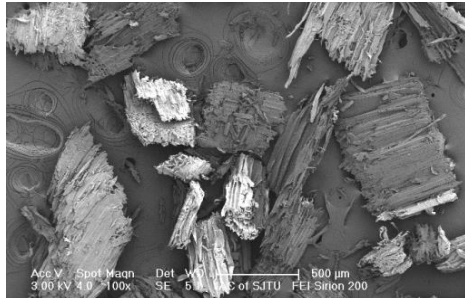


280-300 °C

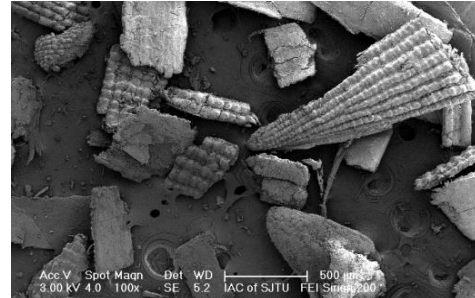
Regarding to the raw materials of sawdust and rice husk, as shown in the Figure 3 (a) and (b), their surface was integrated. But external difference between them was clear. Sawdust is featured by a stack of fibrous structures. And the surface of rice husk is covered with a layer of regular conical convex material. In addition, their sensitivity to the torrefaction is recognizably different in the amplified images by a factor of 1000. No major visible difference can be seen when comparing the images from the raw material of sawdust (Figure 3 (c)) and sawdust treated by torrefaction in 280-300 °C (Figure 3 (d)). However, pronounced surface tears, as an evidence of thermal breakdown, can be observed when comparing the images between the untreated (Figure 3 (e)) and torrefied rice husk in 280-300 °C (Figure 3 (f)). The difference in surface breakdown between sawdust and rice husk may be attributed to the different hemicellulose contents in the two materials. For biomass sample in the torrefaction temperature range of 200–300 °C, mass loss is dominated by dehydration and devolatilization in the reaction regime of hemicellulose component.<sup>6</sup> The release of volatile products during the torrefaction process breaks down the smooth and integrated external epidermis of the biomass. At higher magnification, the phenomenon of surface tears, cracks, cavities, and pores is more significant when comparing the images of the untreated (Figure 3 (g)) and torrefied rice husk in 280-300 °C (Figure 3 (h)).

When the temperature increased, volatiles were released and a deposit was formed on the solid surface partially because of the rapid formation of blockage.<sup>18</sup> Chen *et al.*<sup>19</sup> studied the oxidative torrefaction using two fibrous biomass materials (oil palm fiber and coconut fiber) and two ligneous ones (eucalyptus and cryptomeria japonica) at 300 °C for 1 h with SEM technology. They found that the performance of non-oxidative torrefaction is better than that of oxidative torrefaction. In the

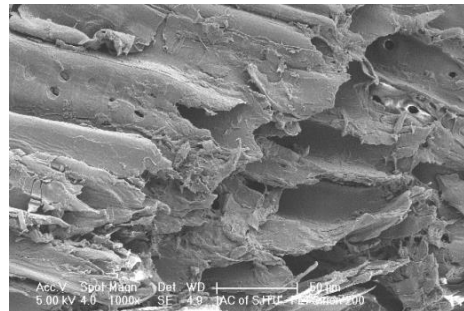
research of Sabil *et al.*,<sup>20</sup> torrefaction has more severe impact on surface structure of empty fruit bunches and palm mesocarp fiber than that of palm kernel shell especially under severe torrefaction conditions revealed by SEM images.



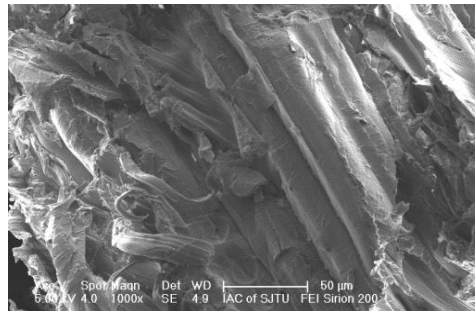
(a)



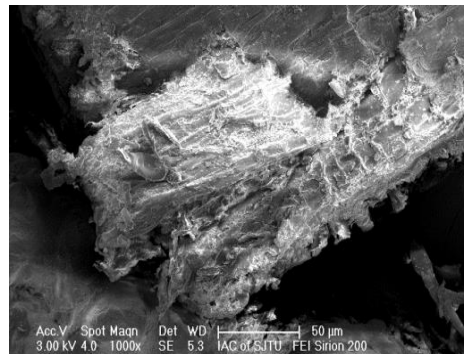
(b)



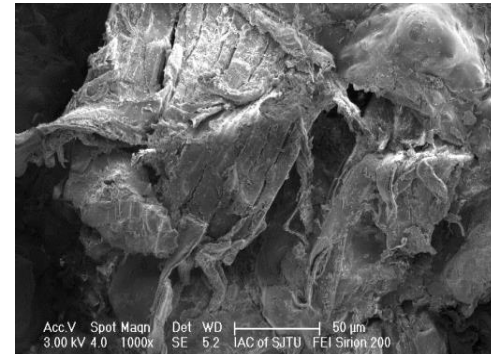
(c)



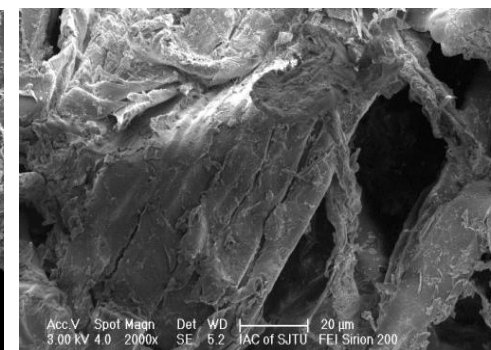
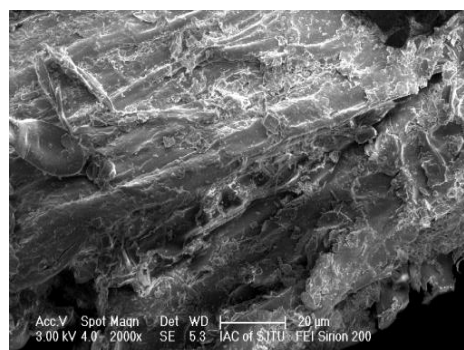
(d)



(e)



(f)



(g)

(h)

Figure 3. SEM micrographs of raw material and torrefied biomass

(a) sawdust, raw material, 100 X; (b) rice husk, raw material, 100 X; (c) sawdust, raw material, 1000 X; (d) sawdust, 280-300 °C, 1000X; (e) rice husk, raw material, 1000 X; (f) rice husk, 280-300 °C, 1000 X; (g) rice husk, raw material, 2000 X; (h) rice husk, 280-300 °C, 2000 X

### 3.2. Weight loss and energy yield

During the process of torrefaction, the weight loss is an important parameter to measure the process evolution. The energy yield is an indicator of the energy lost based on the weight loss and calorific value. The following equations were used to calculate the weight loss (EQ 3) and energy yield (EQ 4):

$$\text{Weight loss} = \frac{M_1 - M_2}{M_1} \times 100\% \quad (\text{EQ 3})$$

$$\text{Energy yield} = \frac{H_2 \cdot M_2}{H_1 \cdot M_1} \times 100\% \quad (\text{EQ 4})$$

where  $M_1$  and  $M_2$  are the weight of the raw material and the weight of the biomass after torrefaction on dry basis, respectively.  $H_1$  represents the HHV value of the raw material and  $H_2$  stands for HHV after torrefaction. Figure 4 shows weight loss of sawdust and rice husk at different torrefaction temperatures.

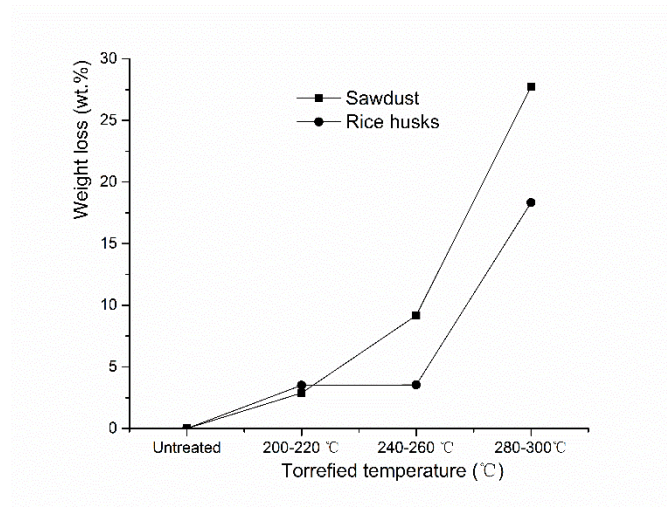


Figure 4. Weight loss of sawdust and rice husk at different torrefaction temperatures

As can be seen in Figure 4, the higher the torrefaction temperature is, the higher the weight loss is. Compared with rice husk, the weight loss of sawdust was more significant in 280-300 °C, where the weight losses were 27.72% and 18.33% for sawdust and rice husk, respectively. However, in the lower temperature of 200-220 °C, rice husk was more sensitive to the temperature variations than sawdust, for the weight loss of rice husk was 3.51% and that of sawdust was 2.88%. In the process of the torrefaction, the weight loss is due to the thermal degradation of the three main components: cellulose, hemicellulose, and lignin, except for the moisture vaporization at a lower temperature. Through the torrefaction process, a portion of the mass is lost, but some favored characters generate.<sup>21</sup> These include improved energetic value, enhanced hydrophobicity, and friability.

The energy yield of sawdust and rice husk at different torrefaction temperatures is plotted in Figure 5. As a whole, the results showed that the energy yield decreased with the increasing of the torrefaction temperature. The influence of temperature on sawdust was more profound than on rice husk, for the energy yields were 77.63% and 89.38% for sawdust and rice husk, respectively, in 280-300 °C. In the research of Yan *et al.*,<sup>22</sup> with increasing temperature, though the mass of the solid decreases, the fuel value of the solid and the quantity of gas increase; in addition, the fuel value of the produced solid may be as much as 36% higher than that of the original biomass. If the HHV of raw biomass is selected as the basis, HHV of the torrefied biomass is enlarged by a factor of 1.07 for sawdust at 280-300 °C. When the rice husk is under the torrefaction process at the same condition, the HHV of the torrefied rice husk is enlarged by a factor of 1.10. Obviously, the slightly intensified HHV from torrefaction is inadequate to offset the weight loss of biomass. However, the hydrophobicity, grindability,<sup>6</sup> pelletability,<sup>23</sup> flowability, and homogeneity characteristics of the biomass are improved, which make the torrefied sample become more storable, combustible, and

attractive for a novel renewable fuel.

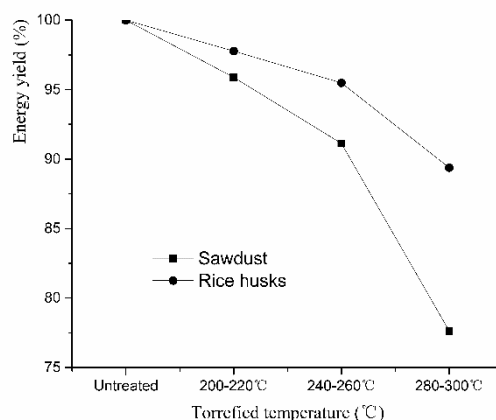


Figure 5. Energy yield of sawdust and rice husk at different torrefaction temperatures

### 3.3. Proximate and ultimate analysis

The physiochemical characteristics of the original and torrefied biomass samples are presented in Table 1. Moisture content is a significant property for the samples. For biomass samples in the experiments (like fast pyrolysis), ignoring any financial consideration, many kinds of methods are used to reduce the moisture content as low as possible, to avoid the fungal degradation during the feedstock storage and transportation, the side reaction caused by water in the original biomass, and the water content ascension in the final products. Through the process of torrefaction, the hygroscopic feature of the raw material is changed to be hydrophobic. The moisture content of the biomass will be decreased dramatically. In addition, the moisture content decreases with the ascent of the temperature. The moisture content of the untreated sawdust was 8.31%. After torrefaction under 280-300 °C, the moisture content was only 0.07%. As for rice husk, the same trend was demonstrated. After the torrefaction, the moisture content of the rice husk in 240-260 °C was 16 times lower than that of the untreated rice husk. As can be seen from Table 1, the torrefaction severity appears to have the most significant impact on the volatile and fixed carbon, and only a minor influence on the ash content. The volatile matter decreased with the increase of torrefaction

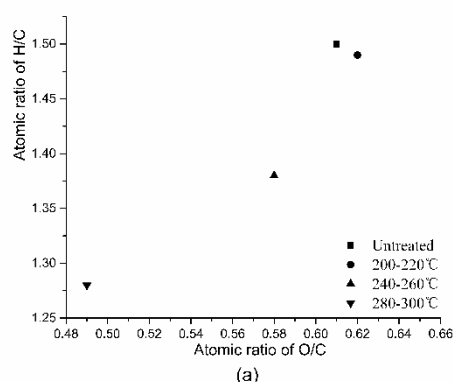
temperature, while the fixed carbon and ash content increased. Increasing the torrefaction temperature will improve the heating value (HHV or LHV) of the biomass. After torrefaction in 280-300 °C, HHV of the sawdust increased from 20.84 MJ/kg to 22.38 MJ/kg, and that of the rice husk increased from 17.07 MJ/kg to 18.68 MJ/kg. In the study of Pimchuai *et al.*,<sup>12</sup> when the agriculture residues ( rice husk, sawdust, peanut husk, bagasse, and water hyacinth) were torrefied at 300 °C for 1.5 h , the highest HHV can be up to 25.68 MJ/kg, which is comparable to the HHV of lignite.

Table 1 Proximate and ultimate analysis of raw materials and torrefied biomass

	Sawdust				Rice Husk			
	Untreated	200-220 °C	240-260 °C	280-300 °C	Untreated	200-220 °C	240-260 °C	280-300 °C
Proximate analysis (wt%)								
Moisture	8.31	1.53	0.83	0.07	9.77	0.85	0.60	0.40
Volatile matter <sup>d.b</sup>	80.74	83.07	75.43	68.53	78.66	64.53	63.38	56.06
Fixed carbon <sup>d.b</sup>	17.84	14.75	22.78	28.44	6.57	20.43	21.85	26.00
Ash <sup>d.b</sup>	1.42	2.18	1.79	3.03	14.77	15.04	14.77	17.94
Heating Value (MJ/kg) <sup>d.b</sup>								
HHV	20.84	20.57	20.90	22.38	17.07	17.29	16.90	18.68
LHV	19.45	19.20	19.60	21.10	15.85	16.11	15.74	17.59
Ultimate analysis (wt%) <sup>d.b</sup>								
C	50.66	50.18	51.80	55.14	42.08	42.99	42.51	46.64
H	6.34	6.25	5.97	5.86	5.55	5.40	5.28	5.01
N	0.13	0.11	0.07	0.06	0.40	0.23	0.20	0.24
O*	41.45	41.28	40.37	35.91	37.2	36.34	37.24	30.17
Inorganic analysis (wt%) <sup>d.b</sup>								
Al	0.01	0.01	—	—	0.01	0.01	—	—
Ca	0.09	0.10	0.12	0.13	0.08	0.11	0.15	0.15
Fe	0.01	0.03	0.01	0.01	0.01	0.02	0.01	0.01
K	0.05	0.05	0.32	0.29	0.04	0.06	0.37	0.39
Mg	0.02	0.02	0.03	0.02	0.02	0.02	0.03	0.03
Mn	—	—	0.03	0.03	—	—	0.04	0.04
Na	0.02	0.03	0.01	0.01	0.01	0.01	0.01	0.01
P	—	0.01	0.03	0.02	—	0.01	0.03	0.03
S	0.01	0.02	0.06	0.05	0.01	0.01	0.07	0.05
Si	0.06	0.06	0.02	0.10	0.28	0.16	0.34	0.22

\* calculated by difference; d.b: dry basis

When the torrefaction condition is intensified, carbon content increases, but hydrogen, nitrogen, and oxygen contents decrease, resulting in decreased atomic hydrogen to carbon ratio and atomic oxygen to carbon ratio. The elemental changes in biomass are often illustrated by Van Krevelen diagram, where H/C index is plotted against O/C. Van Krevelen plot of sawdust and rice husk at different torrefaction temperatures is shown in Figure 6. Normally, the torrefied biomass had lower levels of H/C and O/C ratios than those of original feedstocks. Prior to torrefaction, the sawdust had a H/C of 1.50 and O/C of 0.61. For torrefaction temperature range of 280–300 °C, the H/C ratio dropped to approximately 1.28 and O/C ratio was 0.49. The same trend was observed in the rice husk torrefaction process. The rice husk, a kind of agricultural residue, had a H/C of 1.58 and O/C of 0.66. For torrefaction temperature range of 280–300 °C, the H/C ratio dropped to approximately 1.29 and O/C ratio was 0.49. Reduced moisture content and volatile matter may account for those kinds of changes during the process of the torrefaction, which enhances the pyrolysis, gasification, and combustion properties.<sup>12</sup> And decomposition mechanism of torrefaction involves significant dehydration because the changes in the H/C and O/C atomic ratios of biomass follows the dehydration pathway.<sup>21</sup> The oxygen content loss may be because torrefaction is based on the removal of oxygen from biomass which aims to produce a fuel with increased energy density by decomposing the reactive hemicellulose fraction.<sup>24</sup>



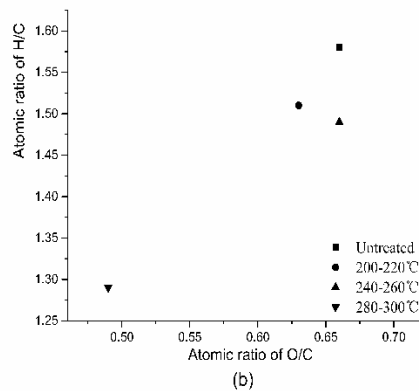


Figure 6. Van Krevelen plot (a) sawdust and (b) rice husk at different torrefaction temperatures

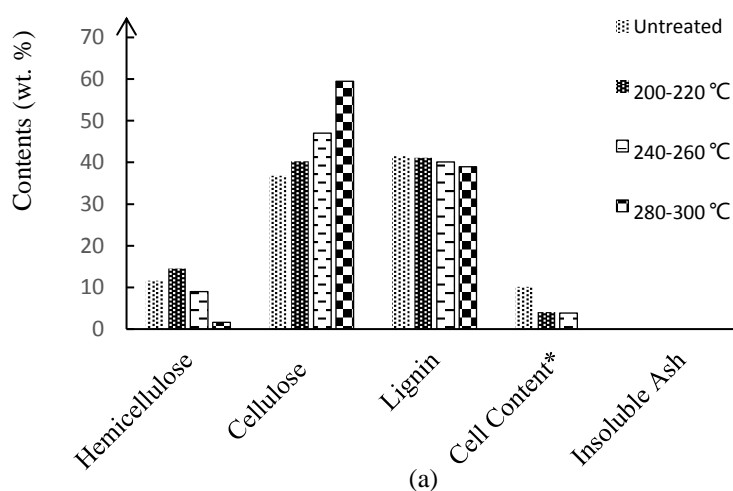
The inorganic content is related to the class of the biomass, fertiliser input, harvest time, and storage duration. Some alkali metals (like sodium, potassium<sup>25</sup>), or inorganic elements like phosphorous<sup>26</sup> influence performance of the fast pyrolysis for they are known to behave as catalysts. So the changes of the inorganic content in the biomass will dramatically affect the performance of the fast pyrolysis. From the Table 1, the calcium and potassium content increased in both biomass feedstocks after torrefaction. What's more, the higher the thermal pre-treatment temperature is, the higher the calcium and potassium content will be. Prior to torrefaction, the calcium and potassium contents of the sawdust were 0.09 wt% and 0.05 wt%, respectively. For torrefaction temperature range of 240-260 °C, the calcium content increased to 0.12 wt% and potassium content to 0.32 wt%. The same trend was observed in the rice husk torrefaction process. The original rice husk had the calcium content of 0.08 wt% and potassium content of 0.04 wt%. After the process of torrefaction in 240-260 °C, the calcium and potassium contents of rice husk were 0.15 wt% and 0.37 wt%, respectively. The highest content of the inorganic element was silica, which can be up to 0.28 wt% in the untreated rice husk. It shows the ascendant trend with the increased torrefied temperature, because in the torrefaction temperature range of 240-260 °C, the silica content is more than that of the untreated biomass. The ash contents of raw sawdust and the torrefied sawdust at 280-300 °C



were 1.42 wt% and 3.03 wt%, respectively. The amount of calcium, potassium, and silica contents of raw sawdust was 0.09, 0.05, and 0.06 wt%, respectively. And that of the torrefied sawdust at 280-300 °C was 0.13, 0.29, 0.10 wt%, respectively. The amount of calcium, potassium, and silica contents of the torrefied sawdust at 280-300 °C increased compared with the raw sawdust. Because at this temperature range, substantial vaporization alkali halides and silica compounds are minor and lots of volatile matter are lost. In the research of Kambo *et al.*,<sup>27</sup> the characteristics of strength, storage, and combustion of miscanthus feedstock were studied under the processes of densification, torrefaction, and hydrothermal carbonization. They found that magnesium content was reduced by 24.38% after the torrefaction pretreatment under 260 °C. Liu *et al.*<sup>28</sup> studied the sodium release and transformation in kitchen waste under torrefaction process and found that sodium release increased with the torrefaction temperature, mainly because of the transformation of a water-soluble form to a CH<sub>3</sub>COONH<sub>4</sub>-soluble form. In this research, the magnesium and sodium content remain constant may because the vaporization of those two elements was approximately equal to the loss of the volatile matter.

The main polymeric structure of the lignocellulosic biomass is hemicellulose, cellulose, and lignin which have different thermal stability. The lignocellulosic components analysis of sawdust and rice husk at different torrefaction temperatures is depicted in Figure 7. During the torrefaction process of the lignocellulosic materials, significant mass loss is associated with the decomposition of hemicellulose. For sawdust in the untreated biomass, the hemicellulose may account for 11.58 wt%. After torrefaction under 280-300 °C, the content of the hemicellulose was only 1.6 wt%. A minor increasing of the hemicellulose content was observed at the torrefaction temperature in 200-220 °C, which may be caused by the dramatically decreasing of the cell content. The more obvious

changes of the hemicellulose content were observed during the rice husk torrefaction process, for there was no hemicellulose detected in the biomass treated after 280-300 °C, and the content of the hemicellulose was changed from 16.62 wt% to less than 0.01 wt%. The cellulose content was steadily increased with the ascendant of the torrefaction temperature in both biomasses. The most abounded component in the untreated sawdust and rice husk was lignin, which accounts for 41.5 wt% and 39.05 wt%, respectively. The content of the lignin experienced slightly changes at the temperature range of torrefaction. Also in the research of Chen *et al.*,<sup>29</sup> the hemicellulose contained in the biomass was destroyed in a significant way, whereas cellulose and lignin were affected only slightly in the light torrefaction. However, in the research of Starace *et al.*,<sup>30</sup> large differences in the fraction of lignin lost during torrefaction were found among feedstocks (southern yellow pine, oak, switchgrass). The difference may be because the feedstock varies in these researches. So cellulose and lignin will play an important role on the utilization of torrefied biomass as a fuel in this research.



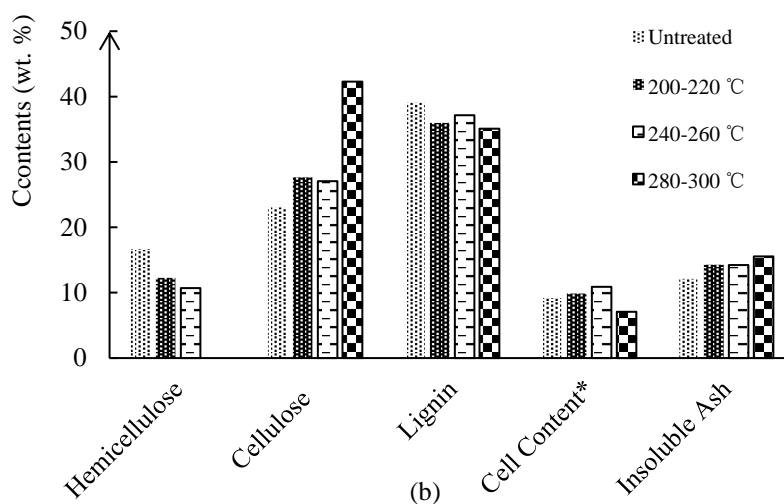


Figure 7. Lignocellulosic components analysis (a) sawdust and (b) rice husk at different torrefaction temperatures

\*Proteins, fat, soluble carbohydrate, and soluble ash

To demonstrate the trends of lignocellulosic components changes through the process of torrefaction clearly, the terms of g per 100 g of untorrefied feedstock were applied to analyze the sawdust composition. Lignin content of the untorrefied sawdust was 41.5 g per 100 g raw sawdust. And after the process of torrefaction of 200-220 °C, lignin content changed to 39.9 g per 100 g raw sawdust. In addition, with the increasing temperature the lignin content was gradually decreased, which were 36.5 g and 28.0 g per 100 g raw sawdust, under 240-260 °C and 280-300 °C, respectively. The same trend was observed in hemicellulose contents changes in the torrefaction pretreatment. Hemicellulose content of the untorrefied sawdust was 11.6 g per 100 g raw sawdust. Though the content of hemicellulose experienced a slightly increase after the torrefaction under 200-220 °C, the hemicellulose content showed the decreasing trend with the increasing of the temperature, for the hemicellulose content was 14.0941 g, 8.2173 g, and 1.152 g per 100 g raw sawdust at the torrefaction temperature 200-220 °C, 240-260 °C, and 280-300 °C, respectively.

### 3.4. Differential thermogravimetric analysis (DTG)

Differential thermogravimetric analysis (DTG) has been widely used in the biomass pyrolysis research,<sup>31</sup> where the derivative weight is defined by the percentage of weight loss per minute. DTG profiles for sawdust and rice husk at different torrefaction temperatures are shown in Figure 8. The higher the torrefaction temperature is, the higher the maximum rate of weight loss is in both kinds of biomass. Because the torrefaction process has changed the tenacious nature of the biomass attributed by the complicated structure, where the hemicellulose matrix bonds the cellulose fibers, and the process has altered the contents of the three main lignocellulosic components (hemicellulose, cellulose, and lignin) and some alkali metals like potassium and sodium which can behave as catalysts. Yang *et al.*<sup>32</sup> found that the weight loss of hemicellulose and cellulose mainly happened at 220-315 °C and 315-400 °C, respectively; and that of lignin at 160-900 °C in a wide temperature range, which was more difficult to decompose. In this research, hemicellulose is the most active for the process of devolatilisation and carbonization which occur at around 250 °C. While at this temperature range, little mass loss is associated with the decomposition of cellulose and lignin. The degradation temperature of cellulose occurs at 270-360 °C and 250-345 °C for sawdust and rice husk, respectively. The process of torrefaction can only slightly change the peak temperature at which the maximum rate of weight loss occurs. For the original sawdust, the peak temperature is 385 °C, while for the torrefied biomass it is 380-385 °C. The same phenomenon was found in rice husk. The peak temperature of rice husk was all between 362-364 °C. Depending on the natures of the tested materials, the weight losses of the tested samples could be classified into three groups:<sup>33</sup> a weakly active reaction, a moderately active reaction, and a strongly active reaction, torrefied at 230 °C, 260 °C and 290 °C, respectively. Some moisture and light volatiles released had a slight impact on

improving the properties of biomass at 230 °C. The properties and heating value of the torrefied biomass could be intensified to a great extent when the biomass torrefied at 260 °C, for some hemicellulose pyrolyzed, whereas little cellulose and lignin were affected. The torrefaction around 290 °C caused a large portion of mass consumed because large amounts of hemicellulose and cellulose were destroyed, so this pre-treatment procedure disadvantaged the torrefied biomass at this temperature range. The pyrolysis behaviors of the torrefied biomass were significantly different from those of the raw materials, for the structure of biomass was changed by the torrefaction and the cross-linking reactions occurred during the pyrolysis process.<sup>34</sup>

Indicated by the weight loss data and TGA results, sawdust is a kind of relatively inactive biomass, and rice husk is one kinds of relatively active biomass in the torrefaction processes. For both kinds of biomass, when the torrefaction condition became severer, the weight loss increased. Most of weight loss associated with the volatile matter. After torrefaction under 280-300 °C, the volatile matter decreased by 12.21% and 21.60%, for sawdust and rice husk, respectively. The relative contents of the hemicellulose decreased with the increased temperature, however, that of the cellulous increased with the torrefaction condition. And the relative contents of the lignin is approximately the same. After torrefaction under 280-300 °C, the hemicellulose content of sawdust changed from 11.58 wt% to 1.6 wt%, while that of rice husk changed from 16.62 wt% to less than 0.01 wt%. Therefore, for both sawdust and rice husk, the peaks indicated the hemicellulose pyrolysis became smaller or even disappeared with the severity of torrefaction in DTG profiles.

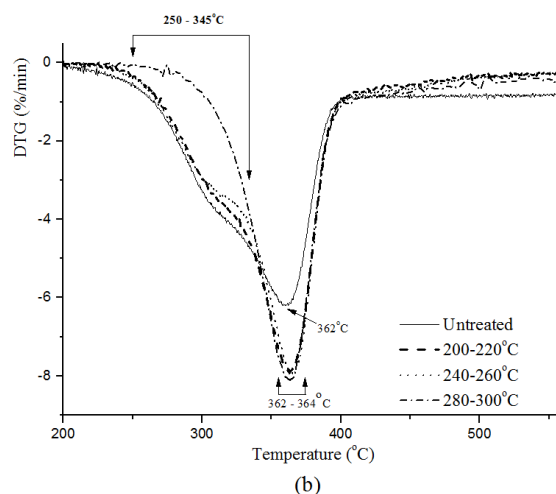
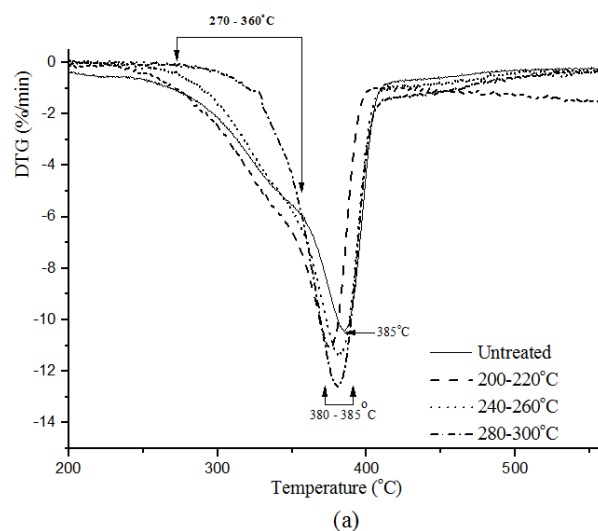


Figure 8. DTG profiles for (a) sawdust and (b) rice husk at different torrefaction temperatures

### 3.5. Py-GC/MS

The thermal decomposition of the original biomass and the biomass treated by torrefaction were studied by Py-GC/MS. Figure 9 shows Py-GC/MS spectrum of sawdust torrefied under 280-300 °C. Table 2 shows relative mass contents of sawdust torrefied under 280-300 °C detected by Py-GC/MS. And in Supporting Information, Py-GC/MS spectrum of sawdust, rice husk, torrefied rice husk under 280-300 °C are shown in Figure S1, Figure S2, Figure S3, respectively. Relative mass contents of sawdust, rice husk, torrefied rice husk under 280-300 °C detected by Py-GC/MS are shown in Table S1, Table S2, Table S3, respectively.

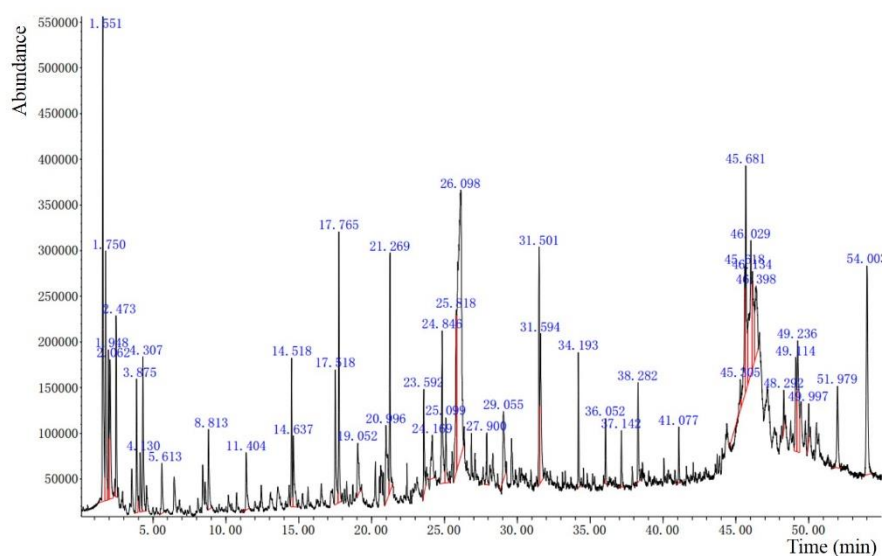


Figure 9. Py-GC/MS spectrum of sawdust torrefied under 280-300 °C

Table 2. Relative mass contents of sawdust torrefied under 280-300 °C detected by Py-GC/MS

	RT (min)	Mass content(%)	Name	CAS No.	Formula	Molar mass
1	1.551	6.24	Carbon dioxide	124-38-9	CO <sub>2</sub>	45
2	1.748	3.23	2,3-Dimethyloxirane	3266-23-7	C <sub>4</sub> H <sub>8</sub> O	72
3	1.946	1.55	1,3-Propanedioic acid	141-82-2	C <sub>3</sub> H <sub>4</sub> O <sub>4</sub>	104
4	2.061	2.68	Acetic acid	64-19-7	C <sub>2</sub> H <sub>4</sub> O <sub>2</sub>	60
5	2.471	1.94	Hydroxyacetone	116-09-6	C <sub>3</sub> H <sub>6</sub> O <sub>2</sub>	74
6	3.877	1.72	Propyl acetate;	109-60-4	C <sub>5</sub> H <sub>10</sub> O <sub>2</sub>	102
7	4.132	0.77	butanedial	638-37-9	C <sub>4</sub> H <sub>6</sub> O <sub>2</sub>	86
8	4.305	2.13	Methyl pyruvate	600-22-6	C <sub>4</sub> H <sub>6</sub> O <sub>3</sub>	102
9	5.615	0.82	Furfural	98—1-1	C <sub>5</sub> H <sub>4</sub> O <sub>2</sub>	96
10	8.813	1.20	2-Cyclopenten-1-one,2-hydroxy-	10493-98-8	C <sub>5</sub> H <sub>6</sub> O <sub>2</sub>	98
11	11.403	0.99	3,4-Dihydroxy-3-cyclobutene-1,2-dione	2892-51-5	C <sub>4</sub> H <sub>2</sub> O <sub>4</sub>	114
12	14.519	1.57	4-Methoxyphenol	150-76-5	C <sub>7</sub> H <sub>8</sub> O <sub>2</sub>	124
13	14.639	1.38	1,2-Dimethylpropylamine	598-74-3	C <sub>5</sub> H <sub>13</sub> N	87
14	17.519	1.92	2,5-Dihydrofuran	1708-29-8	C <sub>4</sub> H <sub>6</sub> O	70
15	17.764	2.98	2-Methoxy-4-methylphenol	93-51-6	C <sub>8</sub> H <sub>10</sub> O <sub>2</sub>	138
16	19.05	1.08	5-Hydroxymethylfurfural	67-47-0	C <sub>6</sub> H <sub>6</sub> O <sub>3</sub>	126
17	22.995	1.98	2-Oxazolidone	497-25-6	C <sub>3</sub> H <sub>5</sub> NO <sub>2</sub>	87
18	21.27	2.64	2-Hydroxy-5-methyl acetophenone	1450-72-2	C <sub>9</sub> H <sub>10</sub> O <sub>2</sub>	150
19	23.591	1.39	Vanillin	121-33-5	C <sub>8</sub> H <sub>8</sub> O <sub>3</sub>	152
20	24.169	1.01	N-Trimethylsilyl-L-alanine trimethylsilyl ester	27844-07-1	C <sub>9</sub> H <sub>23</sub> NO <sub>2</sub> Si <sub>2</sub>	233
21	24.847	2.66	Phenol,2-methoxy-4-(1-propen-1-yl)-	97-54-1	C <sub>10</sub> H <sub>12</sub> O <sub>2</sub>	164
22	25.098	1.04	Homovanillyl alcohol	2380-78-1	C <sub>9</sub> H <sub>12</sub> O <sub>3</sub>	168

23	25.82	2.79	D-Allose	2595-97-3	C <sub>6</sub> H <sub>12</sub> O <sub>6</sub>	180
24	26.099	15.29	1,6-anhydro-beta-d-glucopyranos	498-07-7	C <sub>6</sub> H <sub>10</sub> O <sub>5</sub>	162
25	27.9	0.66	Phenol,4-(3-hydroxy-1-propen-1-yl)-2-methoxy-	458-35-5	C <sub>10</sub> H <sub>12</sub> O <sub>3</sub>	180
26	29.056	1.42	2-Methyl-2-pentenoic acid	3142-72-1	C <sub>6</sub> H <sub>10</sub> O <sub>2</sub>	114
27	31.502	2.72	2-Propenal,3-(4-hydroxy-3-methoxyphenyl)-	458-36-6	C <sub>10</sub> H <sub>10</sub> O <sub>3</sub>	178
28	31.594	2.57	6-Methylnicotinic acid	3222-47-7	C <sub>7</sub> H <sub>7</sub> NO <sub>2</sub>	137
29	34.194	1.98	Diisobutyl phthalate	84-69-5	C <sub>16</sub> H <sub>22</sub> O <sub>4</sub>	278
30	37.141	0.65	Pentane-2,4-dione, 3-(1-adamantyl)	102402-84-6	C <sub>15</sub> H <sub>22</sub> O <sub>2</sub>	234
31	38.282	1.28	4-Ethyl-2-methoxyphenol	2785-89-9	C <sub>9</sub> H <sub>12</sub> O <sub>2</sub>	152
32	41.075	0.59	3,3',5,5'-Tetramethylbenzidine	54827-17-7	C <sub>16</sub> H <sub>20</sub> N <sub>2</sub>	240
33	45.621	2.09	Ethanone, 1-[5-methyl-2-[(4-methylphenyl)amino]-4,6-diphenyl-3-pyridinyl]-1	92630-95-0	—	—
34	45.678	3.58	Tetracyclo[6.3.2.0(2,5).0(1,8)]tridecan-9-ol, 4,4-dimethyl	1000157-75-1	C <sub>15</sub> H <sub>24</sub> O	220
35	46.03	4.43	4-decyl-1,2,3,6,7,8-hexahdropyrene	56247-94-0	C <sub>26</sub> H <sub>36</sub>	349
36	46.136	2.52	1,4-Dioxane-2,5-dimethanol	14236-12-5	C <sub>6</sub> H <sub>12</sub> O <sub>4</sub>	148
37	46.396	2.45	Maleic acid, di-t-butyl ester	18305-60-7	C <sub>12</sub> H <sub>20</sub> O <sub>4</sub>	228
38	48.293	0.52	2-Methoxybenzylamine	6850-57-3	C <sub>8</sub> H <sub>11</sub> NO	137
39	49.117	1.75	3-Ethylamino-4-methylphenol	120-37-6	C <sub>9</sub> H <sub>13</sub> NO	151
40	49.237	2.96	Isolimonene	5113-87-1	C <sub>10</sub> H <sub>16</sub>	136
41	49.998	0.48	5-(4-Amylphenyl)-2-(4-butoxyphenyl)-pyrimidine	144104-95-0	C <sub>25</sub> H <sub>30</sub> N <sub>2</sub> O	375
42	51.997	1.76	1-Decylpyrene	55682-90-1	C <sub>26</sub> H <sub>30</sub>	343
43	54.004	4.80	Indanidine	85392-79-6	C <sub>11</sub> H <sub>13</sub> N <sub>5</sub>	215

All the detected products were classified into 10 groups except carbon dioxide, with the purpose to clarify the compositional changes of the pyrolytic products before and after thermal pretreatment, and the results are presented in Table 3. From the data shown in Table 3, the process of carbonization deeply affects pyrolysis products composition. In addition, thermal pretreatment displayed different capabilities towards the pyrolytic products. For both biomasses, the process of torrefaction reduced the levels of alcohols, ketones, aldehydes, acids, esters, and furans. The carbon dioxide content only slightly altered before and after torrefaction for rice husk. But when sawdust was torrefied, the carbon dioxide reduced from 8.09% to 6.24%. Phenols content in sawdust increased from 13.84%



to 15.68% after torrefaction and for rice husk the phenols content increased from 10.94% to 13.66% after torrefaction. Acids are typically released during torrefaction, which typically results in a decreased acid content after torrefaction relative to an unmodified feedstock. Through the process of torrefaction under 280-300 °C the acids content reduced about 20.4% and 17.9% for sawdust and rice husk, respectively. Anhydrosugars content increased from 3.40% to 18.08% for sawdust after torrefied. None of that was detected in original rice husk and for torrefied rice husk anhydrosugars contents was 10.81%. Anca-Couce *et al.*<sup>35</sup> studied the characterization and condensation behavior of gravimetric tars produced during spruce torrefaction. The tar compounds can be classified into three groups: phenolics, (hetero)cyclic (mainly furans), and non-cyclic (mainly carbonyls). The heavy tars compounds (pyrolytic lignin and sugars) were not identified. In the research of Ru *et al.*,<sup>36</sup> the yields of acids and furans from the pyrolysis of torrefied biomass decreased; the yields of phenols with side branches decreased, but that of phenols without side branches increased, for the lignin side branches were cleaved during high temperature torrefaction. Chen *et al.*<sup>37</sup> found that with increasing torrefaction temperature, the yields of heavier components increased and many chemicals detected in the pyrolysis torrefied biomass can be used as raw materials for valuable chemical products rather than as fuels. Gao *et al.*<sup>38</sup> investigated the pyrolysis and combustion of pine sawdust using TG–FTIR and Py–GC/MS methods, and results showed that the main compounds of pine sawdust thermal decomposition were small molar gases, acetaldehyde, acetic acid, anhydride with formic and acetic anhydride. In this research, small molar gases like carbon dioxide and acids contents were 12.60% and 12.35%, respectively, for original rice husk. When the rice husk was torrefied, the acids content reduced to 10.14%. In the research of Scholze and Meier,<sup>39</sup> the water-insoluble fraction from pyrolysis oil (pyrolytic lignin) was studied by Py–GC/MS and FTIR. They

found that the propyl sidechain has been largely destroyed during the fast pyrolysis process. Zhang *et al.*<sup>40</sup> investigated rice husk under the process of water washing and torrefaction by TGA and Py-GC/MS and also found that acids contents reduced after torrefaction pretreatments.

Table 3 The composition of the pyrolytic products before and after torrefaction

	Sawdust		Rice husk	
	Untreated	280-300 °C	Untreated	280-300 °C
Carbon dioxide (%)	8.09	6.24	12.60	12.61
Alkanes (%)	6.61	4.72	5.74	9.08
Alcohols (%)	5.91	3.56	9.82	5.69
Ketones (%)	13.17	12.74	16.16	11.63
Aldehydes (%)	10.56	4.88	5.95	5.71
Phenols (%)	13.84	15.68	10.94	13.66
Acids (%)	10.58	8.42	12.35	10.14
Esters (%)	10.51	6.84	5.60	4.97
Furans (%)	10.05	3.82	17.79	2.55
Anhydrosugars (%)	3.40	18.08	—	10.81
Others (%)	7.28	15.43	3.06	13.15

### 3.6. Applications

The above results have clearly indicated that the solid fuel properties of the pulverized biomass have been intensified under the process of torrefaction with increased homogeneity and heating value, which facilitates the application of the torrefied biomass as a fuel, especially for fuel pellet production. Rudolfsson *et al.*<sup>41</sup> studied the process optimization of combined biomass torrefaction and fuel pellet production, and the results showed that particle size, torrefaction degree (mass yield), moisture content, and pelletizing temperature had significant influence on the compression and friction work as well as pellet dimensions and strength. In the research of Ulsu *et al.*,<sup>42</sup> the product energy content undergoing the pre-treatment technologies torrefaction combined with pelletisation can be up to 20.4–22.7 GJ/ton, which make the international trade of biomass feasible from the

energy efficiency and economic perspective. Consequently, as a promising thermal pretreatment method, torrefaction can improve the efficiency of biomass as a fuel and promote bioenergy applications.

#### 4. Conclusions

Revealed by the results of surface morphology, weight loss, energy yield, lignocellulose composition, proximate and ultimate analysis, TGA, and Py-GC/MS, thermal pretreatment of sawdust and rice husk by torrefaction has an obvious effects on their physicochemical characteristics and pyrolysis behavior, which indicated that the promising renewable fuel produced by the torrefied biomass.

(1) The biomass structure was dramatically changed after the process of torrefaction. The color of sawdust and rice husk changed from light yellow to dark brown with the increasing torrefaction temperature. Compared to rice husk, sawdust was more sensitive to the increasing temperature indicated by surface morphology analysis. In high temperature, the phenomenon of surface tears, cracks, cavities and pores was more significant.

(2) High temperature had more effects on sawdust than rice husk, for in 280-300 °C the weight losses were 27.72% and 18.33% for sawdust and rice husk, respectively. However, sawdust was observed to be less sensitive in low temperature, compared with rice husk. And the energy yields decreased with the increase of the torrefaction temperature. What's more, energy yield of sawdust was more affected by the process of torrefaction for the energy yields were 77.63% and 89.38% for sawdust and rice husk in 280-300 °C, respectively.

(3) The moisture content of the biomass was decreased dramatically. After torrefaction in 280-300 °C, HHV of the sawdust increased from 20.84 MJ/kg to 22.38 MJ/kg, and that of the rice husk from 17.07 MJ/kg to 18.68 MJ/kg. The significant mass loss was associated with the decomposition

of hemicellulose. The content of the hemicellulose is changed from 16.62 wt% to less than 0.01 wt% for rice husk after torrefied in 280-300 °C.

(4) Hemicellulose was the most reactive material in the process of devolatilisation by lignocellulose composition analysis and TGA. The degradation temperature of cellulose occurred at 270-360 °C and 250-345 °C for sawdust and rice husk, respectively. Py-GC/MS data showed that the process of torrefaction reduced the levels of alcohols, ketones, aldehydes, acids, esters and furans of the pyrolysis products for both kinds of biomass. Phenols content in sawdust was increased from 13.84% to 15.68% after torrefaction, and that for rice husk was increased from 10.94% to 13.66% after torrefaction.

## ■ AUTHOR INFORMATION

Corresponding Author

\* E-mail:liurhou@sjtu.edu.cn

## ■ ACKNOWLEDGEMENTS

Financial support from the National Natural Science Foundation of China through contract (Grant No. 51176121) and Financial support from the EU-China Cooperation for Liquid Fuels from Biomass Pyrolysis (ECOFUEL) under the FP7-PEOPLE- 2009-IRSES are greatly acknowledged. Also, the authors would like to express sincere appreciate to the related analysts from Instrumental Analysis Centre, Shanghai Jiao Tong University for their diligence work.

## ■ REFERENCES

- (1) Lehmann, J., Bio-energy in the black. *Front. Ecol. Environ.* **2007**, 5, (7), 381-387.
- (2) Obersteiner, M.; Azar, C.; Kauppi, P.; Möllersten, K.; Moreira, J.; Nilsson, S.; Read, P.; Riahi, K.; Schlamadinger, B.; Yamagata, Y.; Yan, J., Managing climate risk. *Science*. **2001**, 294, (5543), 786-787.
- (3) Czernik, S.; Bridgwater, A., Overview of applications of biomass fast pyrolysis oil. *Energ. Fuel*. **2004**, 18, (2), 590-598.
- (4) McKendry, P., Energy production from biomass (part 1): overview of biomass. *Bioresource Technol.* **2002**, 83, (1), 37-46.
- (5) Shen, F.; Hu, J.; Zhong, Y.; Liu, M. L.; Saddler, J. N.; Liu, R., Ethanol production from steam-pretreated sweet sorghum bagasse with high substrate consistency enzymatic hydrolysis. *Biomass Bioenerg.* **2012**, 41, 157-164.
- (6) Arias, B.; Pevida, C.; Feroso, J.; Plaza, M.; Rubiera, F.; Pis, J., Influence of torrefaction on the grindability and reactivity of woody biomass. *Fuel Process. Technol.* **2008**, 89, (2), 169-175.
- (7) Strandberg, M.; Olofsson, I.; Pommer, L.; Wiklund-Lindström, S.; Åberg, K.; Nordin, A., Effects of temperature and residence time on continuous torrefaction of spruce wood. *Fuel Process. Technol.* **2015**, 134, 387-398.
- (8) Li, J.; Brzdekiewicz, A.; Yang, W.; Blasiak, W., Co-firing based on biomass torrefaction in a pulverized coal boiler with aim of 100% fuel switching. *Appl. Energy*. **2012**, 99, 344-354.
- (9) Dudyński, M.; van Dyk, J. C.; Kwiatkowski, K.; Sosnowska, M., Biomass gasification: Influence of torrefaction on syngas production and tar formation. *Fuel Process. Technol.* **2015**, 131, 203-212.
- (10) Bach, Q.; Tran, K.; Skreiberg, Ø., Comparative study on the thermal degradation of dry-and wet-torrefied woods. *Appl. Energy*. **2016**.
- (11) Bridgeman, T.; Jones, J.; Shield, I.; Williams, P., Torrefaction of reed canary grass, wheat straw and willow to enhance solid fuel qualities and combustion properties. *Fuel*. **2008**, 87, (6), 844-856.
- (12) Pimchuai, A.; Dutta, A.; Basu, P., Torrefaction of agriculture residue to enhance combustible properties. *Energ. Fuel*. **2010**, 24, (9), 4638-4645.
- (13) Khazraie Shoulaifar, T.; DeMartini, N.; Willför, S.; Pranovich, A.; Smeds, A. I.; Virtanen, T. A. P.; Maunu, S.-L.; Verhoeff, F.; Kiel, J. H.; Hupa, M., Impact of torrefaction on the chemical structure of birch wood. *Energ. Fuel*. **2014**, 28, (6), 3863-3872.
- (14) Prins, M. J.; Ptasinski, K. J.; Janssen, F. J., Torrefaction of wood: Part 1. Weight loss kinetics. *J. Anal. Appl. Pyrol.* **2006**, 77, (1), 28-34.
- (15) Chen, W.; Lu, K.; Tsai, C., An experimental analysis on property and structure variations of agricultural wastes undergoing torrefaction. *Appl. Energy*. **2012**, 100, 318-325.
- (16) Channiwala, S.; Parikh, P., A unified correlation for estimating HHV of solid, liquid and gaseous fuels. *Fuel*. **2002**, 81, (8), 1051-1063.
- (17) Phyllis, database for biomass and waste. Energy Research Center of the Netherlands. *ECN*, 2005.
- (18) Cai, W.; Liu, R., Performance of a commercial-scale biomass fast pyrolysis plant for bio-oil production. *Fuel*. **2016**, 182, 677-686.
- (19) Chen, W.; Lu, K.; Lee, W.; Liu, S.; Lin, T., Non-oxidative and oxidative torrefaction characterization and SEM observations of fibrous and ligneous biomass. *Appl. Energy*. **2014**, 114, 104-113.
- (20) Sabil, K. M.; Aziz, M. A.; Lal, B.; Uemura, Y., Effects of torrefaction on the physiochemical properties of oil palm empty fruit bunches, mesocarp fiber and kernel shell. *Biomass Bioenerg.* **2013**, 56, 351-360.
- (21) Chew, J. J.; Doshi, V., Recent advances in biomass pretreatment–Torrefaction fundamentals and technology. *Renew. Sust. Energy. Rev.* **2011**, 15, (8), 4212-4222.
- (22) Yan, W.; Hastings, J. T.; Acharjee, T. C.; Coronella, C. J.; Vásquez, V. R., Mass and energy balances of

wet torrefaction of lignocellulosic biomass†. *Energ. Fuel.* **2010**, 24, (9), 4738-4742.

(23) Li, H.; Liu, X.; Legros, R.; Bi, X. T.; Lim, C. J.; Sokhansanj, S., Pelletization of torrefied sawdust and properties of torrefied pellets. *Appl. Energy.* **2012**, 93, 680-685.

(24) Van der Stelt, M.; Gerhauser, H.; Kiel, J.; Ptasiński, K., Biomass upgrading by torrefaction for the production of biofuels: A review. *Biomass Bioenerg.* **2011**, 35, (9), 3748-3762.

(25) Shie, J.; Lin, J.; Chang, C.; Lee, D.; Wu, C., Pyrolysis of oil sludge with additives of sodium and potassium compounds. *Resour. conserv. recy.* **2003**, 39, (1), 51-64.

(26) Nowakowski, D. J.; Woodbridge, C. R.; Jones, J. M., Phosphorus catalysis in the pyrolysis behaviour of biomass. *J. Anal. Appl. Pyrol.* **2008**, 83, (2), 197-204.

(27) Kambo, H. S.; Dutta, A., Strength, storage, and combustion characteristics of densified lignocellulosic biomass produced via torrefaction and hydrothermal carbonization. *Appl. Energy.* **2014**, 135, 182-191.

(28) Liu, S.; Qiao, Y.; Lu, Z.; Gui, B.; Wei, M.; Yu, Y.; Xu, M., Release and transformation of sodium in kitchen waste during torrefaction. *Energ. Fuel.* **2014**, 28, (3), 1911-1917.

(29) Chen, W.; Kuo, P., A study on torrefaction of various biomass materials and its impact on lignocellulosic structure simulated by a thermogravimetry. *Energy.* **2010**, 35, (6), 2580-2586.

(30) Starace, A. K.; Evans, R. J.; Lee, D. D.; Carpenter, D. L., Effects of Torrefaction Temperature on Pyrolysis Vapor Products of Woody and Herbaceous Feedstocks. *Energ. Fuel.* **2016**, 30, (7), 5677-5683.

(31) Stenseng, M.; Jensen, A.; Dam-Johansen, K., Investigation of biomass pyrolysis by thermogravimetric analysis and differential scanning calorimetry. *J. Anal. Appl. Pyrol.* **2001**, 58, 765-780.

(32) Yang, H.; Yan, R.; Chen, H.; Lee, D. H.; Zheng, C., Characteristics of hemicellulose, cellulose and lignin pyrolysis. *Fuel.* **2007**, 86, (12), 1781-1788.

(33) Chen, W.; Kuo, P., Torrefaction and co-torrefaction characterization of hemicellulose, cellulose and lignin as well as torrefaction of some basic constituents in biomass. *Energy.* **2011**, 36, (2), 803-811.

(34) Wannapeera, J.; Fungtammasan, B.; Worasuwanarak, N., Effects of temperature and holding time during torrefaction on the pyrolysis behaviors of woody biomass. *J. Anal. Appl. Pyrol.* **2011**, 92, (1), 99-105.

(35) Anca-Couce, A.; Brunner, T.; Kanzian, W.; Obernberger, I.; Trattner, K., Characterization and condensation behaviour of gravimetric tars produced during spruce torrefaction. *J. Anal. Appl. Pyrol.* **2016**, 119, 173-179.

(36) Ru, B.; Wang, S.; Dai, G.; Zhang, L., Effect of torrefaction on biomass physicochemical characteristics and the resulting pyrolysis behavior. *Energ. Fuel.* **2015**, 29, (9), 5865-5874.

(37) Chen, W.; Hsu, H.; Lu, K.; Lee, W.; Lin, T., Thermal pretreatment of wood (Lauan) block by torrefaction and its influence on the properties of the biomass. *Energy.* **2011**, 36, (5), 3012-3021.

(38) Gao, N.; Li, A.; Quan, C.; Du, L.; Duan, Y., TG-FTIR and Py-GC/MS analysis on pyrolysis and combustion of pine sawdust. *J. Anal. Appl. Pyrol.* **2013**, 100, 26-32.

(39) Scholze, B.; Meier, D., Characterization of the water-insoluble fraction from pyrolysis oil (pyrolytic lignin). Part I. PY-GC/MS, FTIR, and functional groups. *J. Anal. Appl. Pyrol.* **2001**, 60, (1), 41-54.

(40) Zhang, S.; Dong, Q.; Zhang, L.; Xiong, Y., Effects of water washing and torrefaction on the pyrolysis behavior and kinetics of rice husk through TGA and Py-GC/MS. *Bioresour. Technol.* **2016**, 199, 352-361.

(41) Rudolfsson, M.; Stelte, W.; Lestander, T. A., Process optimization of combined biomass torrefaction and pelletization for fuel pellet production—A parametric study. *Appl. Energy.* **2015**, 140, 378-384.

(42) Uslu, A.; Faaij, A. P.; Bergman, P. C., Pre-treatment technologies, and their effect on international bioenergy supply chain logistics. Techno-economic evaluation of torrefaction, fast pyrolysis and

pelletisation. *Energy*. **2008**, 33, (8), 1206-1223.

Supporting information:

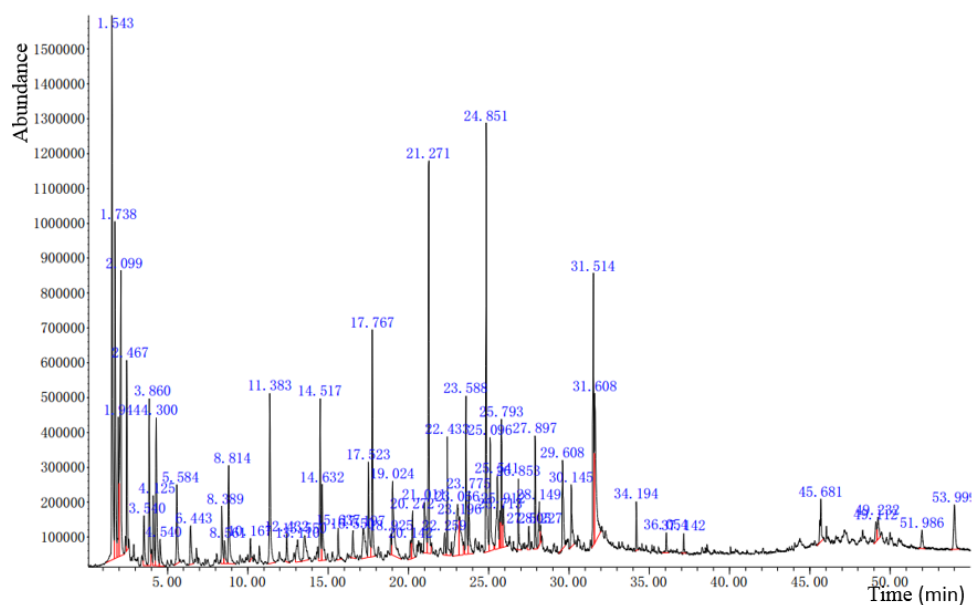


Figure S1. Py-GC/MS spectrum of sawdust

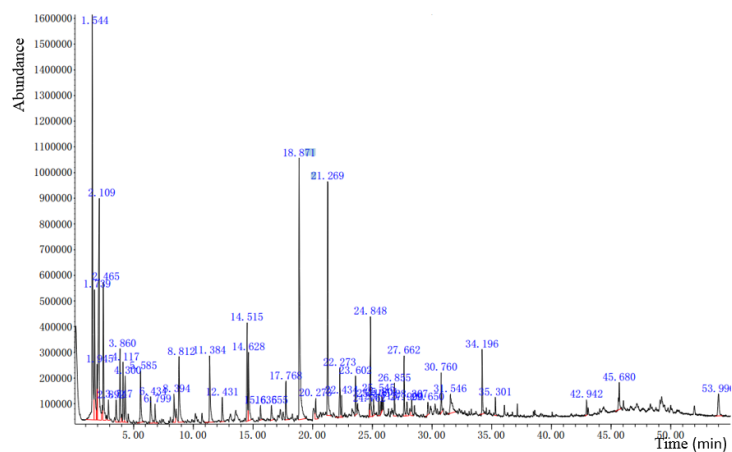


Figure S2. Py-GC/MS spectrum of rice husks

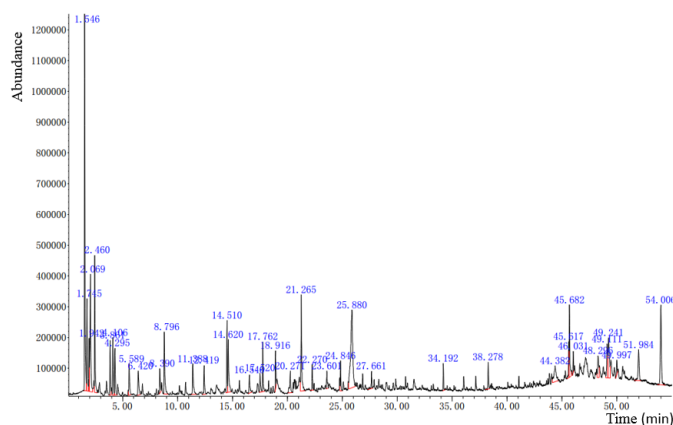


Figure S3. Py-GC/MS spectrum of rice husks torrefied under 280-300 °C

Table S1. Relative mass contents of sawdust detected by Py-GC/MS

	RT	Mass	Name	CAS No.	Formula	Molar
	(min)	content				mass
1	1.542	8.09%	Carbon dioxide	124-38-9	CHO <sub>2</sub>	45
2	1.739	4.43%	Pentane;	109-66-0	C <sub>5</sub> H <sub>12</sub>	72
3	1.946	2.04%	2-Amino-1,3-propanediol;	534-03-2	C <sub>3</sub> H <sub>9</sub> NO <sub>2</sub>	91
4	2.1	4.90%	Acetic acid glacial	64-19-7	C <sub>2</sub> H <sub>4</sub> O <sub>2</sub>	60
5	2.466	2.42%	Hydroxyacetone	116-09-6	C <sub>3</sub> H <sub>6</sub> O <sub>2</sub>	74
6	3.54	0.97%	(E)-2-Methyl-2-butenal	497-03-0	C <sub>5</sub> H <sub>8</sub> O	84
7	3.858	2.43%	Methyl acetate	79-20-9	C <sub>3</sub> H <sub>6</sub> O <sub>2</sub>	74
8	4.123	1.10%	butanedial	638-37-9	C <sub>4</sub> H <sub>6</sub> O <sub>2</sub>	86
9	4.301	2.49%	Methyl pyruvate	600-22-6	C <sub>4</sub> H <sub>6</sub> O <sub>3</sub>	102
10	4.542	0.55%	Oxazole-2-amine	4570-45-0	C <sub>3</sub> H <sub>4</sub> N <sub>2</sub> O	84
11	5.586	1.34%	Furfural	98—1-1	C <sub>5</sub> H <sub>4</sub> O <sub>2</sub>	96
12	6.444	0.87%	Furfuryl alcohol	98-00-0	C <sub>5</sub> H <sub>6</sub> O <sub>2</sub>	98
13	8.389	0.93%	2(5H)-Furanone	497-23-4	C <sub>4</sub> H <sub>4</sub> O <sub>2</sub>	84
14	8.562	0.50%	1-Propene	115-07-1	C <sub>3</sub> H <sub>6</sub>	42
15	8.813	1.79%	1,3-Cyclopentanedione	3859-41-4	C <sub>5</sub> H <sub>6</sub> O <sub>2</sub>	98
16	10.166	0.30%	5-Methyl furfural	620-02-0	C <sub>6</sub> H <sub>6</sub> O <sub>2</sub>	110
17	11.384	2.92%	Oxazolidine, 2,2-diethyl-3-methyl-	161500-43-2	C <sub>8</sub> H <sub>17</sub> NO	143
18	12.434	0.45%	Methyl cyclopentenolone	80-71-7	C <sub>6</sub> H <sub>8</sub> O <sub>2</sub>	112
19	13.113	0.79%	3-Hydroxy-1-methylpiperidine	3554-74-3	C <sub>6</sub> H <sub>13</sub> NO	115
20	13.551	1.02%	4-Hexanolide	695-06-7	C <sub>6</sub> H <sub>10</sub> O <sub>2</sub>	114
21	14.519	2.02%	Guaiacol	90—05-1	C <sub>7</sub> H <sub>8</sub> O <sub>2</sub>	124
22	14.63	1.44%	Pentanal	110-62-3	C <sub>5</sub> H <sub>10</sub> O	86
23	15.636	0.51%	3-Methyl-2,4(3H,5H)-furanone	1192-51-4	C <sub>5</sub> H <sub>6</sub> O <sub>3</sub>	114
24	16.551	0.51%	Oxepane	592-90-5	C <sub>6</sub> H <sub>12</sub> O	100
25	17.196	1.25%	b-Hydroxybutyrolactone	5469-16-9	C <sub>4</sub> H <sub>6</sub> O <sub>3</sub>	102
26	17.524	1.56%	3-Butenoic acid	625-38-7	C <sub>4</sub> H <sub>6</sub> O <sub>2</sub>	86
27	17.769	2.77%	2-Methoxy-4-methylphenol	93-51-6	C <sub>8</sub> H <sub>10</sub> O <sub>2</sub>	138
28	18.925	0.28%	2-Methylbenzaldehyde	529-20-4	C <sub>8</sub> H <sub>8</sub> O	120



29	19.026	2.35%	5-Hydroxymethylfurfural	67-47-0	C6H6O3	126
30	20.143	0.40%	2-Oxobutyric acid	600-18-0	C4H6O3	102
31	20.273	0.86%	4-Ethyl-2-methoxyphenol	2785-89-9	C9H12O2	152
32	21.01	1.45%	Ethylthiocyanate	542-90-5	C3H5NS	87
33	21.27	4.59%	2-Hydroxy-5-methyl acetophenone	1450-72-2	C9H10O2	150
34	22.257	0.35%	3-Ethylbenzaldehyde	34246-54-3	C9H10O	134
35	22.43	1.41%	Eugenol	97-53-0	C10H12O2	164
36	23.066	2.33%	D-Allose	2595-97-3	C6H12O6	180
37	23.196	1.42%	Heptanoic acid	111-14-8	C7H14O2	130
38	23.586	2.45%	Vanillin	121-33-5	C8H8O3	152
39	23.774	1.03%	Phenol,2-methoxy-4-(1-propen-1-yl)-	97-54-1	C10H12O2	164
40	24.853	5.15%	Phenol,2-methoxy-4-(1-propen-1-yl)-	97-54-1	C10H12O2	164
41	25.098	1.87%	Homovanillyl alcohol	2380-78-1	C9H12O3	168
42	25.541	1.80%	1-(2,4,6-trimethylphenyl)-ethanon	1667-01-2	C11H14O	162
43	25.714	0.48%	Benzene, 1,2-diethyl-3,4-dimethyl	54410-75-2	—	—
44	25.791	1.78%	Acetovanillone	498-02-2	C9H10O3	166
45	25.912	1.07%	D-Allose	2595-97-3	C6H12O6	180
46	26.856	0.89%	Ethyl homovanillate	60563-13-5	C11H14O4	210
47	27.506	0.34%	2-(1-cyclohexen-1-yl)-Cyclohexanone	1502-22-3	C12H18O	178
48	27.896	1.43%	2-Isopropyl-3-methoxypyrazine	25773-40-4	C8H12N2O	152
49	28.146	0.79%	Benzeneacetic acid,3,4-dimethoxy-, hydrazide	60075-23-2	C10H14N2O3	210
50	28.228	0.17%	Methyl vanillate	3943-74-6	C9H10O4	182
51	29.605	1.44%	Homovanillic acid	306-08-1	C9H10O4	182
52	30.145	1.21%	Phenol,4-(3-hydroxy-1-propen-1-yl)-2-methoxy-	458-35-5	C10H12O3	180
53	31.512	3.67%	Ferulaldehyde	458-36-6	C10H10O3	178
54	31.608	4.05%	3,7-Benzofurandiol,2,3-dihydro-2,2-dimethyl-	17781-15-6	C10H12O3	180
55	34.194	0.53%	1,2-Benzenedicarboxylic acid bis(2-methylpropyl) ester	84-69-5	C16H22O4	278
56	36.053	0.28%	Dibutyl phthalate	84-74-2	C16H22O4	278
57	37.141	0.22%	2,4,6-Trimethylaniline	88—05-1	C9H13N	135
58	45.684	0.86%	o-Toluic acid, pentadecyl ester	1000292-38-4	—	—
59	49.112	0.41%	2H-Benzocyclohepten-2-one,1,4a,5,6,7,8,9,9a- octahydro-4a-methyl-, trans- (8CI)	17429-26-4	C12H18O	178
60	49.232	0.60%	3-Ethylamino-4-methylphenol	120-37-6	C9H13NO	151
61	51.987	0.45%	Tramazoline	1082-57-1	C13H17N3	215
62	54	1.20%	1-Decylpyrene	55682-90-1	C26H30	343

Table S2. Relative mass contents of rice husk detected by Py-GC/MS

	RT	Mass	Name	CAS No.	Formula	Molar
	(min)	content				mass
1	1.544	12.60%	Carbon dioxide	124-38-9	CO2	44
2	1.739	4.34%	Pentane;	109-66-0	C5H12	72
3	1.945	1.50%	Malonic acid	141-82-2	C3H4O4	104

4	2.109	9.05%	Acetic acid	64-19-7	C2H4O2	60
5	2.465	4.26%	Hydroxyacetone	116-09-6	C3H6O2	74
6	2.892	0.74%	Diethylaminoethanol	100-37-8	C6H15NO	117
7	3.547	0.91%	2-Methylcrotonaldehyde	1115-11-3	C5H8O	84
8	3.86	2.40%	Isobutanol	78-83-1	C4H10O	74
9	4.117	1.88%	butanediol	638-37-9	C4H6O2	86
10	4.3	1.60%	Methyl pyruvate	600-22-6	C4H6O3	102
11	5.585	2.03%	Furfural	98-01-1	C5H4O2	96
12	6.434	1.39%	Furfuryl alcohol	98-00-0	C5H6O2	98
13	6.799	0.71%	Ethyl pyruvate	617-35-6	C5H8O3	116
14	6.799	1.19%	2(5H)-Furanone	497-23-4	C4H4O2	84
15	8.812	2.91%	1,3-Cyclopentanedione	3859-41-4	C5H6O2	98
16	11.384	2.78%	Oxazolidine, 2,2-diethyl-3-methyl-	161500-43-2	C8H17NO	143
17	12.431	0.90%	2-Hydroxy-3-methyl-2-cyclopentenone	80-71-7	C6H8O2	112
18	14.515	2.78%	Guaiacol	90-05-1	C7H8O2	124
19	14.628	2.76%	cyclopropylmethanol	2516-33-8	C4H8O	72
20	15.636	0.48%	3-Methyl-2,4(3H,5H)-furanedione	1192-51-4	C5H6O3	114
21	16.555	0.66%	Barbituric acid	67-52-7	C4H4N2O3	128
22	17.768	1.22%	Phenol, 2-methoxy-4-methyl-	93-51-6	C8H10O2	138
23	18.871	12.71%	2,3-Dihydrobenzofuran	496-16-2	C8H8O	120
24	20.273	0.91%	Phenol, 4-ethyl-2-methoxy-	2785-89-9	C9H12O2	152
25	21.269	6.38%	2-Methoxy-4-vinylphenol	1450-72-2	C9H10O2	150
26	22.273	1.56%	2,6-Dimethoxyphenol	91-10-1	C8H10O3	154
27	22.434	0.58%	Eugenol	97-53-0	C10H12O2	164
28	23.602	1.44%	Isovanillin	621-59-0	C8H8O3	152
29	24.762	0.28%	1,2,4-Trimethoxybenzene	135-77-3	C9H12O3	168
30	24.848	2.77%	(e)-isoeugenol	000097-54-1	C10H12O2	164
31	25.105	0.54%	Homovanillyl alcohol	2380-78-1	C9H12O3	168
32	25.545	0.90%	1-(2,4,5-trimethylphenyl)ethan-1-one	2040-07-5	C11H14O	162
34	25.801	0.38%	Acetovanillone	000498-02-2	C9H10O3	166
35	26.855	1.13%	4-Hydroxy-3-methoxyphenylpyruvic acid	1081-71-6	C10H10O5	210
36	27.662	1.71%	Benzenemethanol, 2-amino-.alpha.-phenyl	13209-38-6	C13H13NO	100
37	27.9	0.62%	3-(4-Hydroxy-3-methoxyphenyl)allyl alcohol	458-35-5	C10H12O3	180
38	28.307	0.65%	Diethyl Phthalate	84-66-2	C12H14O4	222
39	29.65	0.42%	Vanillylacetone	122-48-5	C11H14O3	194
40	30.76	1.12%	Phenol, 2,6-dimethoxy-4-(2-propenyl)-	6627-88-9	C11H14O3	194
41	31.546	1.72%	Coniferaldehyde	458-36-6	C10H10O3	178
42	34.196	1.71%	Diisobutyl phthalate	1000309-04-5	C16H22O4	278
43	35.301	0.49%	Methyl hexadecanoate	112-39-0	C17H34O2	270
44	42.942	0.45%	Adipic acid bis(2-ethylhexyl) ester	103-23-1	C22H42O4	370
45	45.68	1.05%	Benzyl alcohol, 3-ethylamino-	1000158-36-2	—	—
46	53.995	1.40%	Decalin,2-methylene-5,5,8a-trimethyl-1-(2,5-dimethoxybenzyl)- 4a.alpha.	1000195-82-0	—	—

Table S3. Relative mass contents of rice husk torrefied under 280-300 °C detected by Py-GC/MS

	RT	Mass	Name	CAS No.	Formula	Molar
	(min)	content				mass
1	1.544	12.610	Carbon dioxide	124-38-9	CO <sub>2</sub>	44
2	1.744	3.568	2,3-Dimethyloxirane	3266-23-7	C <sub>4</sub> H <sub>8</sub> O	72
3	1.942	1.562	Malonic acid	141-82-2	C <sub>3</sub> H <sub>4</sub> O <sub>4</sub>	104
4	2.069	5.947	Acetic acid glacial	64-19-7	C <sub>2</sub> H <sub>4</sub> O <sub>2</sub>	60
5	2.46	4.823	Isobutanol	78-83-1	C <sub>4</sub> H <sub>10</sub> O	74
6	3.861	2.144	Methyl ethanoate	79-20-9	C <sub>3</sub> H <sub>6</sub> O <sub>2</sub>	74
7	4.106	2.203	butanedial	638-37-9	C <sub>4</sub> H <sub>6</sub> O <sub>2</sub>	86
8	4.295	1.951	Methyl isobutyrate	547-63-7	C <sub>5</sub> H <sub>10</sub> O <sub>2</sub>	102
9	5.589	1.508	Furfural	98-01-1	C <sub>5</sub> H <sub>4</sub> O <sub>2</sub>	96
10	6.42	1.511	2H-Pyran,3,4-dihydro-6-methyl	16015-11-5	C <sub>6</sub> H <sub>10</sub> O	98
11	8.39	1.043	2(5H)-Furanone	497-23-4	C <sub>4</sub> H <sub>4</sub> O <sub>2</sub>	84
12	8.796	2.967	1,3-Cyclopentanedione	3859-41-4	C <sub>5</sub> H <sub>6</sub> O <sub>2</sub>	98
13	11.388	1.796	Phenol	108-95-2	C <sub>6</sub> H <sub>6</sub> O	94
14	12.419	1.373	Methyl cyclopentenolone	80-71-7	C <sub>6</sub> H <sub>8</sub> O <sub>2</sub>	112
15	14.51	2.531	Guaiacol	90-05-1	C <sub>7</sub> H <sub>8</sub> O <sub>2</sub>	124
16	14.62	2.633	Glutaraldehyde	111-30-8	C <sub>5</sub> H <sub>8</sub> O <sub>2</sub>	100
17	16.546	0.963	2-Methylcyclopentanone	1120-72-5	C <sub>6</sub> H <sub>10</sub> O	98
18	17.52	0.894	Aceticacid, ethenyl-	625-38-7	C <sub>4</sub> H <sub>6</sub> O <sub>2</sub>	86
19	17.762	1.768	4-Methyl guaiacol	93-51-6	C <sub>8</sub> H <sub>10</sub> O <sub>2</sub>	138
20	18.916	1.48	propyl-Benzene	103-65-1	C <sub>9</sub> H <sub>12</sub>	120
21	20.271	1.337	4-Ethyl-2-methoxyphenol	2785-89-9	C <sub>9</sub> H <sub>12</sub> O <sub>2</sub>	152
22	21.265	4.484	2-Hydroxy-5-methyl acetophenone	1450-72-2	C <sub>9</sub> H <sub>10</sub> O <sub>2</sub>	150
23	22.27	0.862	Syringol	91-10-1	C <sub>8</sub> H <sub>10</sub> O <sub>3</sub>	154
24	23.601	0.871	Vanillin	121-33-5	C <sub>8</sub> H <sub>8</sub> O <sub>3</sub>	152
25	24.846	1.108	Isoeugenol	97-54-1	C <sub>10</sub> H <sub>12</sub> O <sub>2</sub>	164
26	25.88	10.806	D-Allose	2595-97-3	C <sub>6</sub> H <sub>12</sub> O <sub>6</sub>	180
27	2.661	0.714	3,4-Dimethoxyacetophenone	1131-62-0	C <sub>10</sub> H <sub>12</sub> O <sub>3</sub>	180
28	34.192	0.871	Diisobutyl phthalate	84-69-5	C <sub>16</sub> H <sub>22</sub> O <sub>4</sub>	278
29	38.278	1.048	Homovanillic acid	306-08-1	C <sub>9</sub> H <sub>10</sub> O <sub>4</sub>	182
30	44.382	2.32	2-Methoxy-1-naphthyl thiocyanate	92696-42-9	C <sub>12</sub> H <sub>9</sub> NOS	215
31	45.617	1.133	Ethanone,1-[5-methyl-2-[(4-methylphenyl)amino]-4,6-diphenyl-3-pyridinyl]-	92630-95-0	—	—
32	45.682	3.005	Phenol, 4-amino-2-(1-methylethyl)- (9CI)	16750-66-6	C <sub>9</sub> H <sub>13</sub> NO	151
33	46.031	0.696	Carbamic acid, [4-[(3-cyclohexyl-1-oxopropyl)amino]-2-methoxyphenyl]-, ethyl ester	1000350-13-7	—	—
34	48.296	1.538	Phenol, 3-(ethylamino)-4-methyl-	120-37-6	C <sub>9</sub> H <sub>13</sub> NO	151
35	49.111	1.997	Decalin,2-methylene-5,5,8a-trimethyl-1-(2,5-dimethoxybenzyl)- 4a.alpha.	1000195-82-0	—	—
36	49.241	3.519	Cyclohexane, 1-butenylidene-	36144-40-8	—	—
37	49.997	0.58	3-Ethylamino-4-methylphenol	120-37-6	C <sub>9</sub> H <sub>13</sub> NO	151
38	51.984	2.085	Decalin,2-methylene-5,5,8a-trimethyl-1-(2,5-	1000195-82-0	—	—

---

dimethoxybenzyl)- 4a.alpha.						
39	54.006	5.751	Indanidine	1000337-89-0	C11H13N5	215

---